PRAMANA
— journal of
physics

Vol. 59, No. 6
December 2002
pp. 989–995

An improved injector bunching geometry for ATLAS

RICHARD C PARDO, J BOGATY, B E CLIFFT, S SHEREMENTOV
and P STRICKHORN
Argonne National Laboratory, 9700 S. Cass Avenue, Argonne, IL 60439, USA

Abstract. The bunching system of the ATLAS positive ion injector (PII) has been improved by relocating the harmonic buncher to a point significantly closer to the second stage sine-wave buncher and the injector LINAC. The longitudinal optics design has also been modified and now employs a virtual waist from the harmonic buncher feeding the second stage sine-wave buncher. This geometry improves the handling of space charge for high-current beams, significantly increases the capture fraction into the primary rf bucket and reduces the capture fraction of the unwanted parasitic rf bucket. Total capture and transport through the PII has been demonstrated as high as 80% of the injected dc beam while the population of the parasitic, unwanted rf bucket is typically less than 3% of the total transported beam. To remove this small residual parasitic component a new traveling-wave transmission-line chopper has been developed reducing both transverse and longitudinal emittance growth from the chopping process. This work was supported by the U.S. Department of Energy under contract W-31-109-ENG-38.

Keywords. Positive ion injector; harmonic buncher; beam optics.

PACS Nos 29.17.+w; 41.75.Ak; 29.27.Ac

1. Introduction and original design

The ATLAS bunching system for the positive ion injector (PII) [1] is designed to transform a dc heavy-ion beam from an electron cyclotron resonance (ECR) ion source into a pulsed beam matched to the input of the independently-phased superconducting-resonator PII LINAC. The charge-to-mass ratio of the beams from the ECR sources range from 0.1 to 0.5. This is to be accomplished with minimal emittance growth from the bunching system and must match the acceptance of the LINAC in order to achieve high efficiency and low emittance growth from the acceleration process. This portion of the PII system operates at a fixed beam velocity in order to match the synchronous velocity of the first PII superconducting resonator.

A two-stage bunching process consisting of a first stage multi-frequency harmonic buncher [2] with a fundamental frequency of 12.125 MHz, a second, 24.25 MHz, sine-wave rebuncher and a beam chopper to remove unbunched beam was developed to meet the bunching requirements. The original design of this system placed a three frequency harmonic buncher on the high-voltage platform of the ECR ion source and the rebuncher approximately 1.5 m from the first accelerating structure. In this configuration, the harmonic buncher forms a real time waist just upstream of a 6.0625 MHz sine-wave chopper. The rebuncher reforms that time waist, with a magnification of approximately 1/5, forming

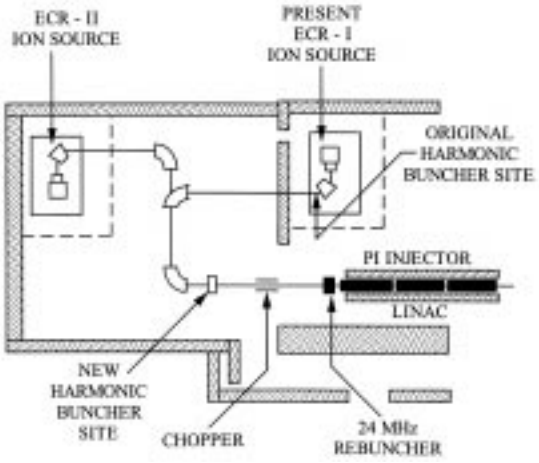

Figure 1. Floor plan of the ATLAS positive ion injector showing the relative location of the components of the injector bunching system.

a time waist just in front of the first accelerating resonator in the LINAC. That configuration is shown in figure 1.

For beam currents less than 1 μA and depending on the exact charge-to-mass ratio (q/m) of the beam, this system is capable of producing a 1.0 to 1.5 ns FWHM time waist from the harmonic buncher and rebunches with the second resonator for acceleration into the LINAC with a width of about 200 to 300 ps. Under these conditions the match into the LINAC allows transmission of 60–65% of the dc beam, comparable to the performance of a similar system used on the ATLAS tandem injector.

In this geometry, the drift distance from the buncher to the first waist is approximately 20 m and the peak voltage required to bunch the beam is typically only few hundred volts. As the beam current increases above 1 μA, space charge forces quickly exceed the bunching voltage required and the compressing charge packet undergoes a 'bounce' prior to actually achieving the bunch waist and the overall bunching performance deteriorates with corresponding poorer matching into the LINAC [3]. This effect is shown in figure 2 for an $^{16}O^{3+}$ beam, which has a q/m ratio similar to many beams used at ATLAS. As can be seen, the effective best bunch quickly becomes unusable as the beam current exceed 5 electrical microamps.

2. Revised configuration

A new configuration of the bunching system has now been implemented. The harmonic buncher has been relocated to a position just past the last bending magnet leading to the PII LINAC. That new configuration is shown also in figure 1. No change in the position of the 24 MHz resonator was required. In addition to the improved handling of space charge effects described below, this new configuration allows the use of only a single bunching system for both the original ECR source and the new ECR-II source shown in figure 1. Also the requirements of a doubly isochronous beam transport to the PII LINAC is eliminated, simplifying beamline tuning.

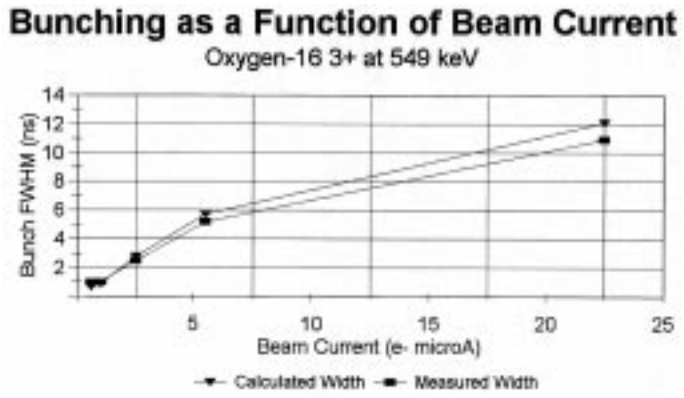

Figure 2. Measured beam bunch width achieved with the three-harmonic buncher on the ECR platform for an $^{16}O^{3+}$ beam as a function of beam current. The results are compared to the calculated bunch width from a simulation with TRACE-3D [4].

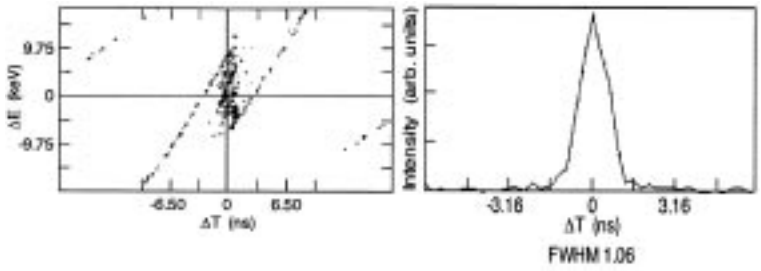

Figure 3. Calculated longitudinal phase ellipse created by a first stage four-harmonic buncher. The harmonic buncher is used to form a real time waist upstream of the sine-wave buncher which will then compress this waist by a factor of 4–5 for injection into the PII LINAC.

This new position provides the opportunity to consider two modes of bunching with the two lens elements – the harmonic buncher and the 24 MHz resonator. One mode forms a real waist just in front of the chopper. This real waist is then reformed with the 24 MHz resonator for injection into the LINAC. The voltages required in this mode are up to 7 kV for the harmonic buncher and 15 kV for the 24 MHz resonator, high but achievable without too much cost. More importantly the distortion in the saw tooth wave form created by the four-harmonic buncher now dominate the beam emittance as shown in figure 3.

The second bunching option uses the harmonic buncher to form a virtual waist at the proper location downstream of the 24 MHz resonator. The second buncher is then used to create a real waist of the proper size and shape at the first accelerating resonator of the LINAC. The voltage requirements are approximately 1/3 of those required for the real waist mode and the distortions from the saw tooth wave form imperfections are correspondingly reduced. The resulting longitudinal emittance is approximately half that of the real waist mode and the expected bunch width injected into the LINAC is also approximately 50% narrower than the real waist mode. These effects can be seen by comparing the real waist results shown in figure 3 and the virtual waist results shown in figure 4.

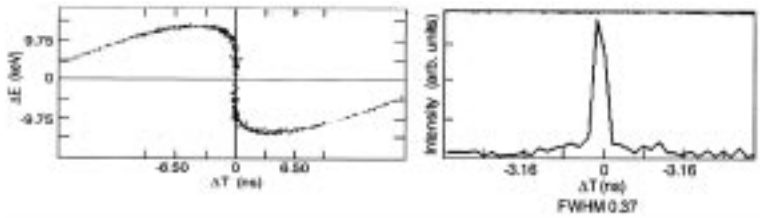

Figure 4. Calculated longitudinal phase ellipse created by the combined effects of a first stage four-harmonic buncher and a second stage sine-wave buncher. The harmonic buncher is used to form a virtual time waist downstream of the sine wave buncher. The distortions visible in figure 3 from the imperfect harmonic buncher wave form are not visible in this simulation. The emittance is dominated by the source system energy spread and the distortions are due to the sine-wave buncher.

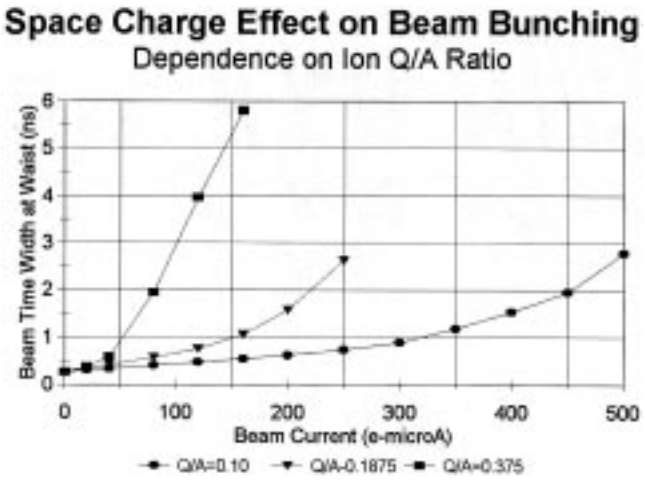

Figure 5. Calculated bunch width as a function of total beam current and as a function of ion species charge-to-mass ratio for the new PII bunching geometry. The ability to handle higher beam currents in this system has been improved by at least an order of magnitude.

The expected improvement in performance of this bunching geometry is quite dramatic. Figure 5 shows the calculated bunch width from the harmonic buncher as a function of beam current for three different beam q/m ratios. Only the highest charge-state beams are expected to have beam current limitations due to poor bunching.

3. Transmission-line traveling-wave chopper

Approximately 30% of the original dc beam is not bunched acceptably and must be removed. That task falls to the beam chopper. In the original system geometry, a time waist is formed near the chopper. In this mode the transmitted beam has a small time width as

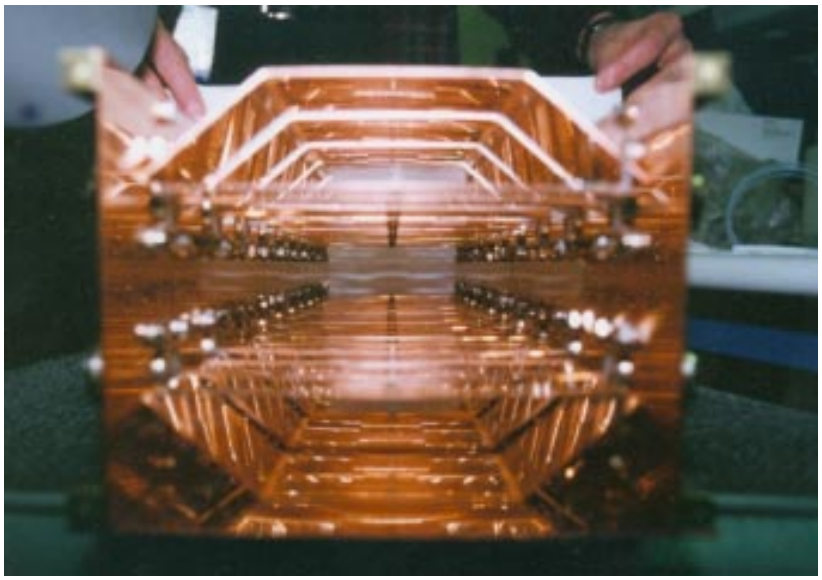

Figure 6. Electrode structure of transmission-line traveling-wave chopper.

the bunch traverses the chopper and is relatively undisturbed as the chopper deflects the unbunched beam component. Even in this mode a sine-wave chopper slightly deflects the bunch tails alternately up and down causing 10–20% transverse emittance growth. In the new geometry, the bunch has only been compressed by a factor of 2.7 as the bunch crosses the chopper location and so is still approximately 30 ns wide. Under this new condition, the emittance growth induced by a sine-wave chopper is quite large and unacceptable.

A transmission-line traveling-wave chopper [5] has been developed in order to handle this new bunching situation. Such a chopper creates a square-wave, zero-voltage transmission window which propagates in phase through the chopper, transmitting the desired bunch without deflection and with minimal transverse and longitudinal distortions. The physical design of the chopper electrode structure and electronic properties are shown in figure 6.

The chopper consists of 10 deflecting electrodes arranged as part of a 125Ω transmission line. Alternated with the chopping electrodes are field clamping ground electrodes, which can also be given a dc bias to correct for small non-zero voltage offsets of the transmitting voltage window. The chopping electrodes are well-matched into the transmission line minimizing pulse distortions and reflections. The electrodes are 1.5 cm long in the beam propagation direction and 9 cm wide. The electrodes centers are spaced apart by 4.5 cm and, at an ion velocity of 0.0085 c, separated in time by 17.14 ns by delay line sections. The total length of the electrode structure is 45 cm.

The maximum voltage required for sufficient beam deflection is approximately 1 kV but typical voltage requirements are less than 500 V. At 500 V, the CW power requirement is 1 kW when operated at the required frequency of 12.125 MHz. The chopper wave form at 500 V is shown in figure 7.

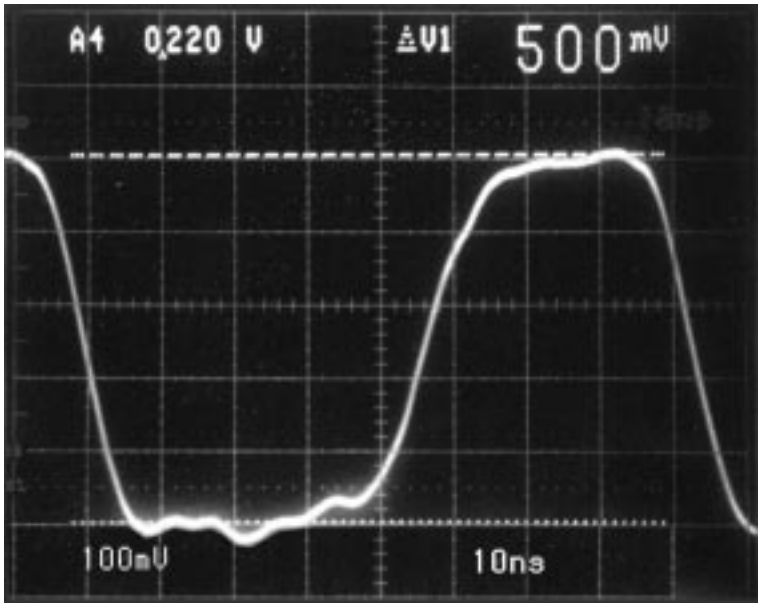

Figure 7. Chopper wave form with deflection voltage set for 500 V. The transmission window is 35 ns wide and fall time is approximately 10 ns.

Table 1. Measured vertical emittance growth for different bunching and chopping conditions.

Bunch width (ns)	Chopper type	Horizontal emittance ε_n^x (π mm·mr)	Vertical emittance ε_n^y (π mm·mr)
3.0	None	0.10	0.10
3.0	Sine	0.10	0.13
18.0	Sine	0.10	0.17
3.0	TWC	0.10	0.10
18.0	TWC	0.10	0.12

4. Results

The new bunching system discussed here is now in full operation. The total beam accepted by the LINAC with the new bunching geometry is now approximately 80% of the dc beam. Transmission of the chopper-transmitted beam has been as good as 100% through the PII LINAC. This is to be compared to a maximum transmission of 60–65% of the dc beam with the old bunching system. In addition a slight improvement in the percentage of remaining beam captured in the intermediate rf bucket by the sine-wave buncher is observed. Previously 8% of the transmitted beam was captured in the intermediate rf bucket. The new virtual waist geometry has reduced this value to 2.5%.

The improvement in handling high beam currents is best demonstrated so far with the test acceleration of a 105 electrical microamp beam of $^{84}Kr^{14+}$ $(q/A = 0.17)$ through the PII LINAC with 75% transmission. This test shows that the match into the PII LINAC has not been worsened even at this high current.

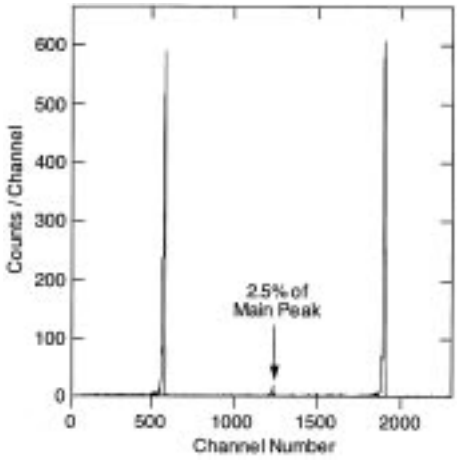

Figure 8. Beam time distribution after acceleration without the transmission-line traveling-wave chopper in use. Note both the satellite peak between the two main bunches as well as the improperly accelerated continuum beam tails.

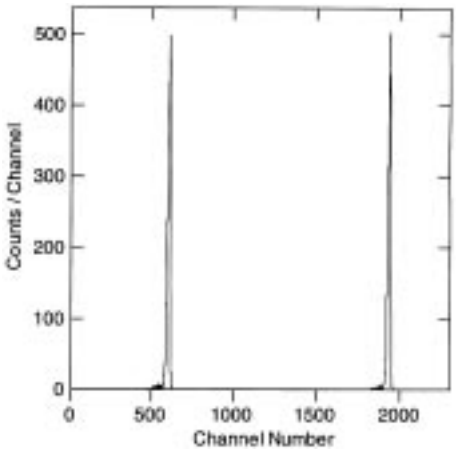

Figure 9. Beam time distribution after acceleration with the transmission-line traveling-wave chopper on. The satellite beam peak has been removed as well as the unbunched continuum tails.

A comparison of measured emittance growth in the original sine-wave chopper and the new traveling-wave chopper is given in table 1. The data show that even for bunch widths of 3 ns FWHM, the sine-wave chopper induces a 30% emittance growth, but that for an 18 ns wide pulse the transverse emittance growth is only 20%. This data was taken with only a 20 ns wide window. For the actual operating condition the bunch width is approximately 30 ns and the voltage window has been widened to 35 ns. Therefore we expect that we are achieving similar performance in the actual operation, but that has not been experimentally determined at this time.

The bunch time distribution after acceleration in the PII LINAC is shown in figures 8 and 9 with and without the chopper in operation. One can see that the satellite peak captured by the sine-wave buncher is removed as well as the continuum timing tails from improperly accelerated, unbunched beam components.

References

[1] L M Bollinger *et al*, *Nucl. Instrum. Methods* **B79**, 753 (1993)
[2] F J Lynch *et al*, *Nucl. Instrum. Methods* **159**, 245 (1979)
[3] R C Pardo and R Smith, *Proc. 1995 Particle Accelerator Conference and International Conference on High-energy Accelerators*, Dallas, TX, 1–5 May 1995, IEEE, 0-7803-3053, **3**, 1849 (1996)
[4] K R Crandall, *Trace 3-D Documentation*, Los Alamos National Laboratory, LA-11054-MS (August 1987)
[5] R C Pardo, J M Bogaty and B E Clifft, *Proc. 1998 Linear Accelerator Conf.*, ANL-98/28, Vol. 2, 998 (1999)